过程分析技术在干法制粒条带性质测量中的应用进展

杨亚光[1,2,3], 安广涛[1,2,3], 闫 媛[1,2,3], 赵 玉[1,2,3], 吴驿瑶[1,2,3], 祁东利[1,2,3*]

(1. 天津中医药大学, 现代中药创制全国重点实验室, 天津 301617; 2. 天津中医药大学, 现代中药发现与制剂技术教育部工程研究中心, 天津 301617; 3. 天津中医药大学中医药研究院, 天津 301617)

摘要: 干法制粒是一种机械化程度较高的药物颗粒制备方法, 其中辊压制粒是较为常用的干法制粒方法, 辊压条带的制备是干法制粒中的关键步骤, 条带的性质, 例如密度、固体分数及孔隙率等, 决定颗粒的成型率等性质, 显著影响颗粒的质量。条带性质的常规测定方法, 离线且耗时长, 已无法满足连续生产的需求。而新兴的过程分析技术能够在线实时检测条带性质, 结合数据分析技术, 可反馈、控制和改进条带制备过程, 获得高质量条带, 有利支撑辊压制粒连续生产。基于过程分析技术的条带性质检测方法取得显著进展, 已成为辊压制粒过程分析和控制研究热点。本文系统总结条带性质的常规测定方法和过程分析方法的最新研究进展, 以期对辊压条带性质监测和辊压制粒连续生产提供理论指导。

关键词: 干法制粒; 辊压条带; 药物颗粒; 过程分析技术; 近红外光谱; 近红外化学成像; 红外热成像

中图分类号: R943 **文献标识码**: A **文章编号**: 0513-4870(2026)02-0453-12

Advances in the application of process analytical technology in the measurement of ribbon properties in roller compaction dry granulation

YANG Ya-guang[1,2,3], AN Guang-tao[1,2,3], YAN Yuan[1,2,3], ZHAO Yu[1,2,3], WU Yi-yao[1,2,3], QI Dong-li[1,2,3*]

(*1. State Key Laboratory of Chinese Medicine Modernization, Tianjin University of Traditional Chinese Medicine, Tianjin 301617, China; 2. Engineering Research Center of Modern Chinese Medicine Discovery and Preparation Technique, Ministry of Education, Tianjin University of Traditional Chinese Medicine, Tianjin 301617, China; 3. Institute of Traditional Chinese Medicine, Tianjin University of Traditional Chinese Medicine, Tianjin 301617, China*)

Abstract: Dry granulation is a highly mechanized method for the preparation of drug granules. Roller compaction is a commonly used dry granulation method. The preparation of roller-compacted ribbons is a key step in dry granulation, and the properties of ribbons, such as density, solid fraction, and porosity, is related to the formation rate of drug granules, and directly determine their quality. The conventional method for measuring ribbons properties, which is off-line and time-consuming, can no longer meet the needs of continuous production. The emerging process analysis technology is capable of online real-time detection of ribbons properties. Combined with data analysis technology, it can provide feedback, control, and improve the ribbons preparation process to obtain high-quality ribbons, which is beneficial for continuous production of roller compaction. The method of detecting ribbon properties based on process analysis technology has made significant progress, and has become a hot topic in the analysis and control of roller compaction processes. This article systematically summarizes the latest progress in conventional determination methods and process analysis methods of ribbon properties, in order

收稿日期: 2025-03-24; 修回日期: 2025-08-11.
基金项目: 天津市教委科技项目−重点项目 (2022ZD040).
*通讯作者 Tel: 86-22-59791991, E-mail: qidongli@tjutcm.edu.cn
DOI: 10.16438/j.0513-4870.2025-0314

to provide theoretical guidance for the monitoring of ribbon properties and the continuous production of roller compaction dry granulation.

Key words: dry granulation; roller-compacted ribbon; drug granule; process analysis technology; near-infrared spectroscopy; near-infrared chemical imaging; infrared thermal imaging

干法制粒是指将药粉与辅料混匀, 不用液态黏合剂, 经辊轮压制成大片或条带后, 破碎整粒成粒度适中、流动性好的颗粒的方法[1]。干法制粒借助挤压力促使粉末黏合成型, 不仅避免药物与水发生降解反应, 也没有干燥过程, 不发生药物受热分解, 制粒过程机械化程度高、绿色节能, 尤其适用于遇水不稳定及热不稳定的药物[2-4], 因此在制药产业中得到广泛应用。

干法制粒可分为重压制粒、气动干法制粒和辊压制粒, 其中气动干法制粒作为一种新型的干法制粒技术, 可生产具有良好流动性和压缩性的颗粒[5-7]。辊压制粒能够准确地控制物料的辊压时间, 具有更好的生产能力[8]。辊压制粒分为两个关键步骤: ① 辊压实, 粉末在两个反向旋转的光滑辊或者滚花辊之间挤压形成条带; ② 条带铣削, 条带研磨破碎转化为颗粒。辊压条带决定颗粒的成型率、粒度分布、细粉量和含量均匀性等关键性质, 并在后续片剂连续生产的过程中影响片剂的质量。因此, 测量辊压条带性质可判断条带质量, 优化和控制干法制粒过程, 保证颗粒和片剂的质量。

目前已报道的辊压条带性质有包络密度[9,10], 固体分数[11]和孔隙率[12,13]。条带性质的测量有常规方法、离线方法和在线方法。常规方法是条带性质测量的参考方法, 但其测量时间长, 效率低且实验结果滞后。连续生产重视制剂过程, 需要实时监测过程信息, 来保证最终制剂的质量[14]。过程分析技术 (process analysis technology, PAT) 实时收集、分析、反馈、控制制剂过程, 并持续改进药物制剂生产过程中的关键质量属性, 为制剂生产提供了过程控制工具[15-17]。基于 PAT 的条带性质离线和在线测量方法纷纷建立和应用, 提高了条带性质的分析质量, 加速了干法制粒的过程控制和工艺研究, 取得了明显的进步, 然而缺乏相关总结。

本文将综述干法制粒过程中条带性质的常规测量方法和最新离线、在线的过程分析方法的研究进展, 为条带测量和干法制粒过程研究提供理论基础。

1 条带性质测量的常规方法

条带性质的常规测量包括粉末体积位移法, 汞侵入法, 吸油法, 卡尺法。常规方法是条带性质测量的参考方法, 常作为过程分析技术研究中的参考方法, 验证离线和在线过程分析工具的适用性以及预测的准确性。表 1 给出了条带测量常规方法的仪器、优势以及不足。

1.1 条带密度的测定

条带密度是条带的重量与体积之比, 常使用包络密度 ($\rho_{envelop}$) 或堆积密度 (ρ_{bulk}) 来表示, 反映了条带材料的致密程度。因为条带的形态不规则、表面粗糙, 所以测定其包络体积是条带密度测定的关键。粉末体积位移法使用一种微型刚性球体作为准流体介质包裹条带不规则表面, 在轻微抖动状态下通过活塞推动介质与条带紧密贴合而不进入条带内部空隙, 以测量前、后的活塞位移差值来确定样品的包络体积[9,18] (图 1A), 再结合天平称量得到的条带重量, 来计算条带的包络密度。

Table1 Instruments, advantages, and disadvantages of conventional methods of roller compacted ribbons

Conventional method	Ribbon property	Instrument	Advantage	Disadvantage
Powder volume displacement method	Envelope density, porosity	Envelope density analyzer; in conjunction with a densitometry, the solid fraction and porosity of the sample can be calculated	Rapid and accurate determination of the volume and density of irregular samples, which is the most authoritative and accurate envelope density determination instrument at present	The price of the instrument is relatively expensive, and it is rarely used in ribbon determination experiments in China
Caliper method	Bulk density ρ_{bulk}	Caliper	Simple and fast measurement	It is only suitable for the ribbon with regular shapes, and is not suitable for measuring irregular and curved samples, and the measurement error is large
Mercury intrusion porosimetry	Porosity	Mercury intrusion porosimeter	It is a more popular measurement method at present, and the measurement results are accurate and reliable	The test time is long, liquid metal mercury is toxic, and there may be safety risks
Oil absorption method	Porosity	Vacuum drying oven, liquid paraffin oil, petri dish, true density meter	The determination method is relatively simple and convenient, the cost is low, and the results are more accurate and reliable	The measurement time is long, and the operation process is cumbersome

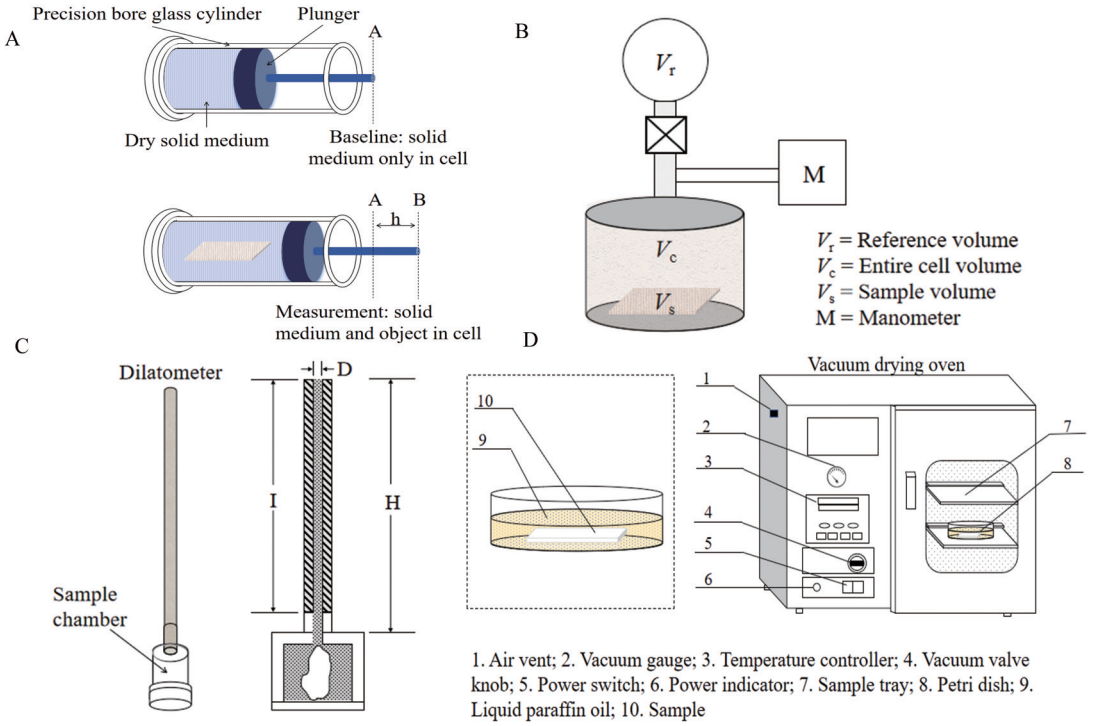


Figure 1 Schematic diagram of the determination of the properties of the ribbon. A: Demonstration of powder volume displacement method; B: Schematic diagram of gas specific gravity method; C: Mercury porosiometer dilatometer; D: Schematic diagram of the sample measured by the oil absorption method

1.2 真密度的测定

真密度 (ρ_{true}), 又称真实密度或密度, 是去除物料内部孔隙或者颗粒间空隙后的密度。气体比重法常作为真密度测定的方法, 所用设备是氦气气体置换真密度仪 (图 1B)[18,19]。分析前预先称量条带的重量, 条带的体积通过测量由条带置换的气体体积来确定, 条带重量和体积之比即为条带的真密度 ρ_{true}。该方法条带体积测量流程如下: 把条带置于测试池中, 密封, 打开连接参考体积和测试单元的阀门, 压力计显示为系统参考压力。然后关闭该阀门, 使参考体积与测试单元分离。测试单元用测量气体加压至初始压力。然后关闭该阀门, 将参考体积与测试单元连接, 压力降至最终压力。根据公式 (1) 计算条带体积 (V_s):

$$V_s = V_c - \frac{V_r}{\left[\frac{P_i - P_r}{P_f - P_r}\right] - 1} \quad (1)$$

其中, V_c 为空池体积, V_r 为参考体积, P_i 为初始压力, P_f 为最终压力, P_r 为系统参考压力。

根据公式 (2) 计算样品的密度。

$$\rho_{true} = w/V_s \quad (2)$$

1.3 条带固体分数/孔隙率 (ε) 的测定

固体分数 (solid fraction, SF) 是条带中固体的体积分数, 可由条带的包络密度与真密度之比计算而得[20,21], 见公式 (3):

$$SF = \rho_{envelop}/\rho_{true} \quad (3)$$

孔隙率 (porosity, ε) 表示条带中空隙的体积分数, 可由汞侵入法或吸油法测定。孔隙率和固体分数的关系[22]见公式 (4):

$$\varepsilon = 1 - SF \quad (4)$$

1.3.1 粉末体积位移法 该方法首先测量条带的包络密度 (见 1.1 项), 再结合真密度数据 (见 1.2 项), 可根据公式 (3) 算出条带的固体分数, 进而根据公式 (4) 计算条带的孔隙率。该方法适用于多种形状和尺寸的条带样品, 可重复测试。

1.3.2 卡尺法 卡尺法使用分辨率为 0.01 mm 的卡尺, 测量条带的长度、宽度和厚度, 计算出条带的体积, 结合条带重量数据, 可计算出条带的密度, 再结合真密度数据, 可获得固体分数或孔隙率结果。并通过公式 $\rho_{bulk} = m/V$ 计算。卡尺法要求条带形状规整光滑, 所以并不适用于测定滚花条带或弯曲条带的孔隙率[20]。

1.3.3 汞侵入法 汞侵入法是测量孔隙率的常用技术, 也是公认的参考方法[23], 该方法使用压汞孔隙度仪 (压汞仪), 其原理是基于汞在孔隙中的润湿性和不可压缩性, 通过加压使汞进入条带的孔隙中, 进而测量孔隙的体积和分布。开始前将条带样品置于膨胀计中 (图 1C), 分析天平称量载样膨胀计组件, 将组件逐

步进行低压和高压分析, 最后进行数据分析, 获得孔体积数据[12], 孔体积与条带体积之比即为条带孔隙率。

1.3.4 吸油法 相对于压汞法, 吸油法可提供一种较为安全的孔隙率测量方法。在吸油法中, 首先用真密度仪测定条带样品真密度, 条带重量除以真密度得到条带体积, 随后将条带放入含有液体石蜡油的培养皿中; 将培养皿转移到真空干燥器中, 维持真空 15 min; 释放真空, 让样品将油吸收到其内部孔隙中 30 min (图 1D); 用纸巾小心地擦拭条带去除多余的油; 对含油饱和条带进行称重, 并利用条带的增重 (最终为含油体积) 和含油密度估算孔隙体积[12,13]。根据公式 (5) 计算吸油法的条带孔隙率 ($\varepsilon_{\text{oil absorption}}$):

$$\varepsilon_{\text{oil absorption}} = [V_{\text{oil}} / (V_{\text{oil}} + V_{\text{ribbon}})] \times 100\% \quad (5)$$

其中, V_{oil}为吸油体积, V_{ribbon}为条带体积。

2 离线过程分析工具用于条带性质表征

条带的过程分析技术有近红外光谱 (near-infrared spectroscopy, NIRS), 近红外化学成像 (near-infrared chemical imaging, NIR-CI)、太赫兹光谱 (terahertz spectroscopy, THz)、红外热成像 (infrared thermography, IRT)、激光热导和 X 射线显微计算机断层扫描 (X-ray computed microtomography, XμCT)[24]等, 这些技术依据应用方式可分为离线和在线两种。将其离线或者在线数据与常规参考方法测定的数据相结合, 运用化学计量学或者其他数据分析方法, 建立起两类数据的关系校准曲线或者条带性质的预测模型。通过曲线或模型, 过程分析技术用于条带性质的分析。通常按难易程度先开展离线过程分析研究, 再开展在线过程分析研究。表 2 给出了常用的条带过程分析技术的原理、表征方法、应用优势、局限性等内容。

2.1 基于光谱学的离线检测技术

2.1.1 NIRS 测定包络密度 NIRS 技术是一种基于化学成分官能团在近红外光谱区域的吸收特性来提取样品的化学成分、物理性质等信息的技术, 具有快速、准确、无损、成本小的特点, 已经广泛应用于制药过程

Table 2 Principles, characterization methods, application advantages, and limitations of process analytical technologies. NIRS: Near-infrared spectroscopy; PLS: Partial least squares; PCA: Principal component analysis; NIR-CI: Near-infrared chemical imaging; IRT: Infrared thermography; THz: Terahertz spectroscopy; XμCT: X-ray computed microtomography; LT: Laser triangulation; GASMAS: Gas in scattering media absorption spectroscopy

Process analytical technique	Ribbon characteristic	Principle	Characterization method	Application benefit	Limitation
NIRS	Envelope density	Vibrational absorption of chemical bonds	Chemometric modeling, such as PLS and PCA, etc	Rapid and non-destructive characterization of sample envelope density	The signal-to-noise ratio is low, the spectral peaks overlap, and the presence of multiple components in the near-infrared spectroscopy sample will interfere with the spectral signal
NIR-CI	Porosity	Hyperspectral imaging obtains spectral information and spatial information of samples	Second derivative preprocessing PLS modeling	The near-infrared chemical spectrogram has high spatial resolution and can be used to characterize the physical properties of multi-component samples	Limited to surface analysis, and principal component analysis is required for dimensionality reduction
IRT	Envelope density, solid fraction	Thermal radiation detection on the surface of the ribbon	Modeling based on Newton's law of cooling	Millisecond-level response, strong process relevance	It is significantly affected by environmental temperature
THz	Density, porosity	The refractive index of the ribbon is associated with the density of the sample	Refractive index and density model	Sample characterization is fast and lossless, with high resolution	The cost of equipment is relatively high
XμCT	Density, porosity	X-ray penetration causes attenuation in the sample ($I_x = I_0 e^{\mu x}$)	Density calibration of sample grayscale values	Three-dimensional visualization, high spatial resolution, multi-property synchronous detection	Scans are time-consuming and cannot be characterized quickly
LT	Solid fraction	3D point cloud reconstruction of sample irregular volume	Volume integration determines the sample envelope volume	Non-contact measurement, full coverage calculation of ribbon volume, high accuracy, short measurement time	The surface of the ribbon needs to have a certain refractive index, and the volume measurement error of the low-density ribbon is large
GASMAS	Porosity	Gas absorption spectroscopy, determination of the path length of photons in the solid phase and gas phase	Correlation analysis between optical porosity and physical porosity	The single measurement speed is fast and the detection accuracy is high	The presence of measurable gas molecules in the sample is required, and the rough surface will increase the scattering noise

中[25,26], 但是NIRS吸收强度较弱、信噪比低、谱峰重叠严重, 无法直接用于定性或定量分析, 需采用化学计量学[27,28]的方法将待测样品的NIRS与其物理化学性质进行关联, 建立数学模型后方可预测待测样品的组成和性质[29-31]。在条带密度表征方面, 研究者们以NIRS作为分析工具, 以常规条带密度测定方法作为参考方法, 验证了NIRS可作为一种新的过程分析工具无损表征条带的密度, 图2A简述了NIRS表征条带密度的过程。

McAuliffe等[18]构建离线NIRS密度预测模型, 将得到的反射率数据转换为吸光度, 通过标准正态变量变换结合光谱均值中心化, 证实了离线近红外光谱与条带包络密度之间具有良好的相关性, 为在线监测奠定了关键理论基础。Crowley等[9]发现了辊压条带质量波动影响近红外光谱精准测量, 采用视觉丢弃法和33%修剪平均值法除去错误光谱数据, 增强了NIRS在辊压过程中在线监测的适用性。

2.1.2 NIR-CI测定孔隙率 近红外化学成像是在近红外光谱技术的基础上, 结合成像技术发展起来的一种检测条带性质的技术, 其原理基于物质在近红外光谱区域的吸收特性, 通过光谱技术获得待测区域内的光谱数据集, 获取样品的光谱信息和空间信息, 即超立方阵 (图2B), 像元表征单一空间点的连续光谱特征, 像平面反映所有空间点在特定波长下的强度响应。通过选择特定像元或像平面, 可分别提取局部光谱信息或全局空间响应[32,33]。结合孔隙率常规测定数据, 建立孔隙率预测模型。近红外化学成像仪由光源、成像系统、分光系统、检测器、数据采集和处理系统组成(图2C)[34], NIR-CI技术常用于鉴别片剂表面成分及辅料的分布、片剂的溶解、粉末混合均匀度等[35-37]。

Lim等[19]以微晶纤维素 (microcrystalline cellulose, MCC) 为原料, 进行单组分近红外化学成像表征研究, 对辊压条带采用离线近红外化学成像扫描, 根据公式(6) 计算反射率 (R):

$$R = (S - D)/(B - D) \quad (6)$$

其中, S为样本图像立方体的反射率, D为暗图像立方体的反射率, B为背景图像立方体的反射率。对光谱进行二阶导数预处理, 可以有效减少条带不平整表面所引起的基线效应, 提高模型的准确性。实验显示, 条带单点孔隙率值与平均吸光度具有线性关系, 相关性为0.925 8, 表明所建立的模型对孔隙率的预测良好。Khorasani等[12]对辊压条带进行离线NIR-CI分析。以吸油法为参考方法, 建立了条带的偏最小二乘 (partial least squares, PLS) 回归模型。结果表明, PLS模型可以解释条带孔隙率99.5%以上的变异, 预测孔隙率的变化。

NIR-CI光谱与化学计量学相结合, 所开发的基于NIR-CI的模型可用于监测辊压实过程中的条带孔隙率, 并且NIR-CI是一种非破坏性工具, 可实现过程可视化, 从而更好地了解辊压条带的过程[13,38]。

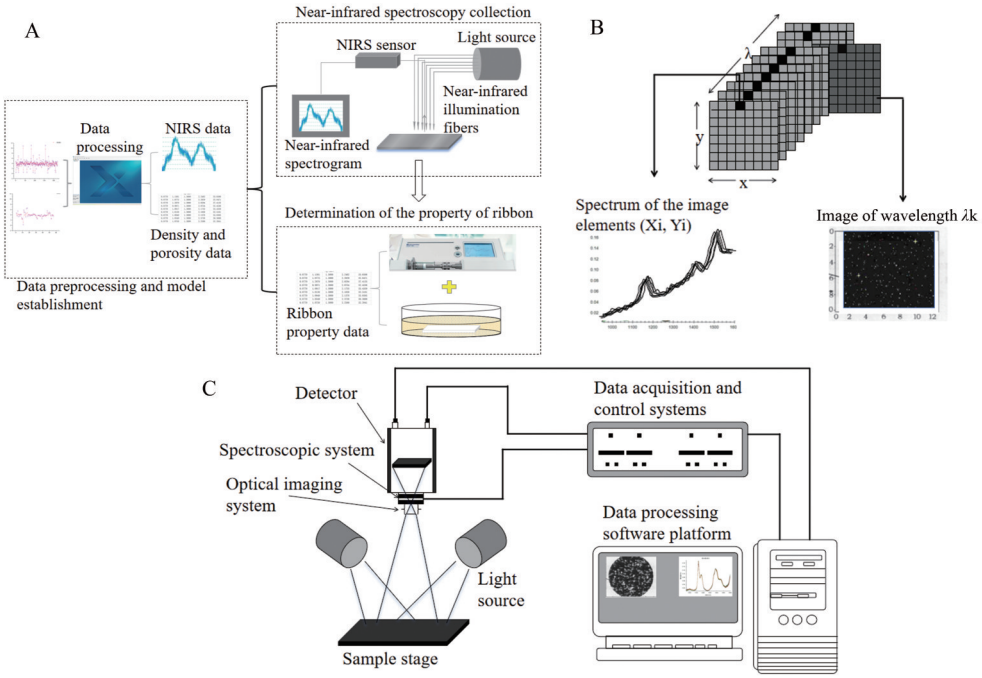


Figure 2 Spectroscopy-based offline detection. A: Flow chart of near-infrared spectroscopy model establishment; B: Schematic diagram of the cube matrix for near-infrared chemical imaging; C: Schematic diagram of near-infrared chemical imaging instruments

2.1.3 太赫兹光谱测定密度和孔隙率 太赫兹波兼具光子与电子特性, 具有非破坏性、材料穿透性强、安全性高和分辨率高等优势[39]。太赫兹脉冲成像 (terahertz pulsed imaging, TPI) 和太赫兹时域光谱 (terahertz time-domain spectroscopy, THz-TDS) 技术通过脉冲太赫兹波与物质相互作用, 获得待测样品反射或透射的光谱信息, 再将太赫兹时域上振幅和相位信息用傅里叶变换为折射率和吸收系数等频域波形特征。通过建立域波形特征与待测样品性质关联模型, 实现药物材料及固体制剂的物理性质表征[40-43], 成为条带密度和孔隙率表征的重要离线分析工具。

Zhang 等[24]利用 TPI 法研究条带密度的变化, 实验结果表明, TPI 测得的条带平均折射率与其堆积密度成线性关系, 据此建立了不同材料的条带折射率与密度的方程, 根据条带折射率计算堆积密度。Dong 等[44]开发了一种使用 THz-TDS 测量条带孔隙率的新方法, 激光传感器测量条带厚度 (*H*), 在同一点进行太赫兹透射, 根据公式 (7) 计算样品的有效折射率 (n_{eff}):

$$n_{eff} = c\Delta t + 1 \quad (7)$$

其中, Δt 是参考信号和样本信号之间的太赫兹脉冲的时间延迟, c 为光在真空中的速度, 1 是空气的折射率。样品的孔隙率 (此处为 f) 与有效折射率相关:

$$n_{eff} = n_{solid} + (1 - n_{solid})\, f \quad (8)$$

其中, n_{solid} 是样品在零孔隙率下的固有折射率, 而该数据是未知的, 因此需要进行校准测量建立折射率与孔隙率的线性相关。实验结果表明, 太赫兹测量的条带孔隙率与粉末体积位移参考方法高度一致。

2.2 基于热力学与成像的离线检测技术

2.2.1 IRT 测定密度 红外辐射是从温度高于 0 K 的物体表面发射出来的电磁辐射, 其强度和波长取决于表面温度, 因此, 根据红外辐射可以得到物体表面温度[45]。红外热成像仪利用红外探测器和光学成像物镜来接收被测目标的红外辐射能量, 内部的光敏元件能将红外辐射能量转换为电信号, 并形成清晰的热图像, 这些热图像以不同的颜色表示被测样品的温度分布, 从而能直观地观察到被测样品的整体温度状况, 也可用于评估材料的性质 (如密度、孔隙率等)[46], 因此 IRT 技术也被应用于辊压条带的性质表征。

Omar 等[47]使用热成像仪监测辊压过程中条带从辊隙中离开时的温度信息 (图 3A)。研究发现, 辊压过程中条带的表面温度随着辊轮间隙增大、辊轮速度增加而升高。热图像不仅反映条带的表面温度, 也反映了不同工艺参数下条带的性质变化。Wiedey 等[48]利用红外热成像仪记录 MCC 条带离开辊轮间隙的温度变化过程, 不仅发现了条带表面温度与其密度具有正相关关系 ($R > 0.98$); 还根据“牛顿冷却定律”, 获得条带温度冷却方程:

$$dT/dt = j \times \Delta T \quad (9)$$

其中, dT/dt 为不同时间的条带温度, j 为温度冷却常数, ΔT 为表面温度与环境温度之差。

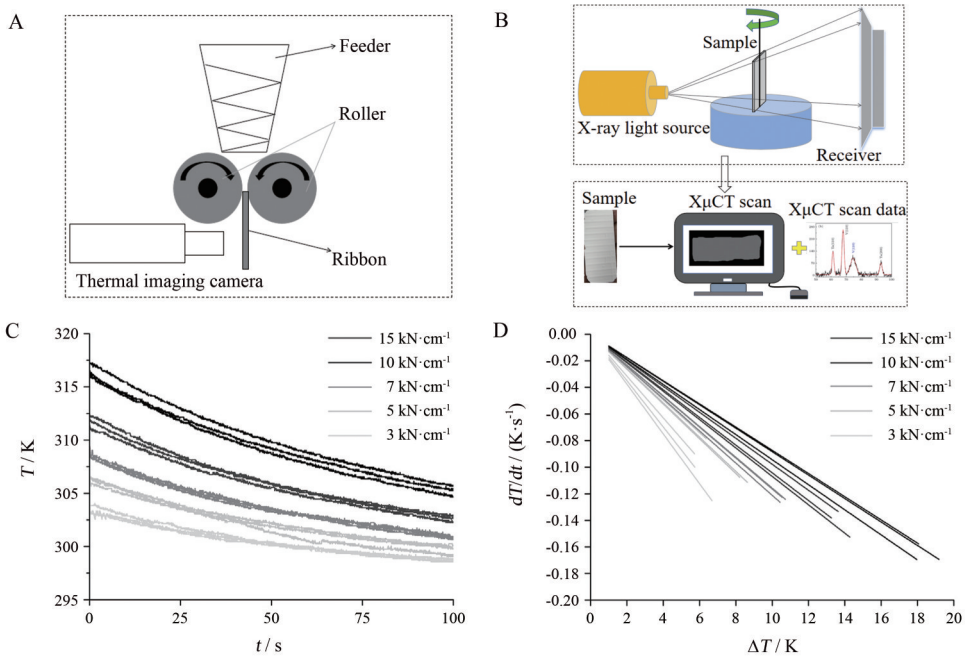


Figure 3 Thermodynamic and imaging-based offline detection. A: Schematic diagram of the thermal imager setup; B: Schematic diagram of the XμCT scan sample; C: Cooling curve plot of the ribbons; D: Cooling rate of ribbons against ΔT[48]. Adapted from Ref. 48 with permission. Copyright © 2018 Powder Technology

通过绘制条带的冷却曲线和dT/dt对ΔT的函数图像 (图3C、D), 发现条带的冷却速率与条带的密度相关, 因此条带密度不仅可以根据条带温度来计算, 也可以根据条带温度冷却速率来计算。红外热成像仪测定条带密度具有很好的适用性, 不仅测温时间很短, 还能及时反映工艺变化对条带密度的影响, 在长期实验中条带密度数值稳定, 而且适用于不同物料, 包括辅料MCC、添加助流剂和润滑剂的各种处方混合物等[49]。

2.2.2 X射线显微计算机断层扫描测定密度 X射线显微计算机断层扫描 (X-ray microcomputed tomography, XμCT) 是根据X射线穿过材料时发生衰减的原理而设计的一种无损成像技术, 其空间分辨率可以达到微米级的水平。该技术广泛应用于土壤、地质分析、岩石检测, 中药材鉴定、中药片剂表征等领域, 在制药领域XμCT还可对固体制剂的性质进行表征[50-56]。当射线束穿过被检测物体时, 入射光线强度由于物质吸收发生衰减, 探测器接收穿过物体的X光。射线穿过物体后的强度衰减与物质密度、结构相关, 故可根据衰减特征计算物体的密度、孔隙率等结构信息[57-59]。而在干法制粒领域也开发了对条带密度表征的XμCT方法。

样品台用于固定和调节物体, 软件系统生成物体二维切片图及三维数据。XμCT方法是一种非破坏性的测量样品密度的方法, 基于穿过物体的X射线的衰减方程为[20]:

$$I_x = I_0 e^{-\mu x} \tag{10}$$

其中, x是物体到射线源的距离, I_x是光束在距离x处穿过物体后的强度, μ是线性衰减系数, 它是质量衰减系数和样品密度的乘积。

由于给定材料的质量衰减系数是恒定的, μ与样品密度呈线性关系。因此, 由灰度值表示测量强度I_x, 并建立与样品密度的函数, 依据灰度值和样品密度之间的线性关系, 可通过灰度值测定条带的密度, XμCT是条带密度测定的一种参考方法, 可校准离线或者在线过程分析技术的数据。

Omar等[47]使用XμCT扫描乳糖材质的条带, 用Image J软件分析所得的X射线图像 (图3B)。图像中的黑色像素表示空气 (孔隙), 白色像素表示粉末。以黑色像素数 (空气) 和总像素数 (空气和粉末) 的比率代表条带的孔隙率。Wiedey等[4]以三维图像的灰度值表征条带在长度、宽度和厚度方向上的密度分布, 每次扫描前, 都将液压压片机制备的校准片剂添加到扫描中, 获取校准曲线, 从而把灰度值转化为密度分布。Miguélez-Morán等[60]应用切片法、微压痕法和XμCT法对辊压条带的密度分布进行研究, 使用X射线图像像素值校准条带密度, 不仅可以清晰展现条带的密度整体分布情况, 还可以获得更详细的局部密度分布信息。但XμCT法并不适合检测多组分混合物条带的密度, 因为混合物的密度和化学成分都会影响X射线衰减系数, 从而影响CT图像的像素值。

2.3 基于光学的离线检测技术

2.3.1 激光三角法离线测量条带固体分数 激光三角测量法 (laser triangulation, LT) 是利用光学反射规律和相似三角形原理 (图4A), 通过激光投射、散射光成像及信号处理实现长度、体积等性质的非接触式测量[61,62]。LT方法能对复杂的三维曲面进行快速准确的非接触式测量, 在工业中的长度、距离以及三维形貌等检测中有着广泛应用[63-65]。LT法测量长度依据Scheimpflug条件[66], 建立长度测量方程:

$$y = \frac{a_0 x \sin\beta}{b_0 \sin\alpha - x\sin(\alpha + \beta)} \tag{11}$$

其中, y是所测长度位移, x是光斑位移, α为入射光与反射光的夹角, β为反射光与CCD光敏面夹角, a_0是O点成像物距, b_0是O点成像像距。

基于LT原理的测量装置 (图4C) 通过平移扫描获取样品三维形貌数据[67], 系统工作时, LT传感器与相机沿X轴移动, 通过图像处理提取激光中心线各点的高度 (ΔH_i) 及Y轴坐标 (Y_i), 生成三维点云 (X_i, Y_i, ΔH_i)。基于点云数据, 采用积分算法计算样品体积, 并实现三维可视化。

Lillotte等[21]基于LT原理研究了一种新型的分析设备VS100 (图4B), 评估其作为条带性质表征的离线过程分析工具的适用性, 通过两个LT传感器扫描样品的上下两面, 两个三维点云经过软件处理后产生样品的表面模型, 组合这些模型生成样品的全封闭表面模型, 根据该表面模型计算样品体积, 样品的质量由分析天平测定, 由此计算样品的密度。

以XμCT法和粉末体积位移法作为参考方法。结果显示, LT法与XμCT法、粉末体积位移法测量数据具有良好的相关性和一致性, 且测量精度高, 时间最短, 仅为3.5 min, 是一种可靠的条带密度离线分析方法。

2.3.2 GASMAS测量条带光学孔隙率 气体散射介质吸收光谱 (gas in scattering media absorption spectroscopy, GASMAS) 是一种基于可调谐二极管激光吸收光谱原理的先进检测技术。该技术使用激光照射样品, 通过GASMAS检测激光吸收, 得到穿过样品空隙中空气的距离, 使用飞行时间光谱测量光传播的总距离, 这两个距离测量值之比为“光学孔隙率”(optical porosity, Φ_{OPT}), 其公式为:

$$\Phi_{OPT} = L_{gas}/L_{tot} \tag{12}$$

其中, L_{tot}表示光子穿过气–固复合体系的总平均

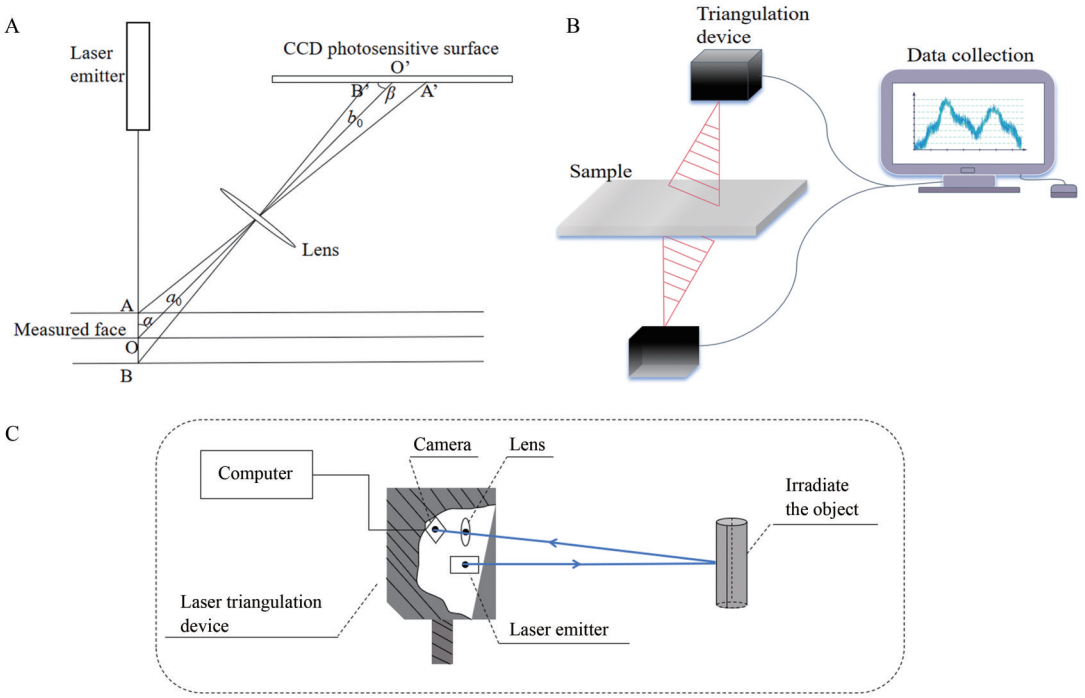


Figure 4 Detection based on laser triangulation. A: Laser triangulation principle optical path diagram; B: Schematic diagram of the LT device (VS100) scan; C: Diagram of a device based on laser triangulation

路径长度, L_{gas}则对应光子仅通过孔隙中气体相的路径长度。该技术已经应用于多孔材料[68]和条带孔隙率[69]的预测。

Johansson 等[69]使用 GASMAS 测量通过孔的路径长度, 飞行时间光谱测量光通过样品的平均飞行时间, 飞行时间除以平均折射率 (包括孔隙中的空气) 转换为L_{tot}, 根据公式 (12) 计算出光学孔隙度。将测量所得的光学孔隙率与物理孔隙率进行相关性分析, 两者存在良好的一致性, 测量数据和理论预测数据十分吻合。

GASMAS 法引入“光学孔隙率”这一概念, 提出了一种新的表征条带孔隙率的方法, 该方法不需要大量校准, 具有良好的应用前景, 但该仪器目前还处在离线测定的研究阶段, 还需进一步研究其在干法制粒生产线的在线应用, 提高其应用范围。

3 过程分析技术用于在线条带性质测量

过程分析技术从离线到在线过程的转变, 需要建立离线光谱校准模型, 因为在线监测时条带质量波动, 会生成可变的近红外光谱数据, 这增加了光谱的筛选、分析和解释的难度, 所以条带在线监测更具挑战性。

3.1 近红外光谱在线监测条带性质

NIRS 技术近年来在条带性质在线监测领域取得突破性进展。McAuliffe 等[18]采用多点近红外分光光度计, 实现了条带密度的在线动态监测 (图 5A)。通过光谱积分与粉末体积位移法的关联研究, 发现近红外光谱与条带密度间存在显著相关性 (pearson 相关系数 $r = 0.880$), 为建立实时密度反馈控制系统奠定了理论基础, 对今后过程分析技术应用于条带密度的监测和控制提供了新的在线监测手段。

Acevedo 等[70]阐明了 MCC 条带的近红外光谱斜率与密度呈高度线性相关 ($r = 0.981\ 2$), 同时构建了基于 1 120～1 310 nm 和 1 305～2 205 nm 双波长区域的密度预测模型, 发现高波长区域 (1 305～2 205 nm) 模型预测精度显著优于低波长区, 这一发现为传感器波长选择提供了重要依据。Samanta 等[71]采用近红外光谱实时监测条带, 采用 PLS 回归技术建立药物含量的全局预测模型, 抗张强度、杨氏模量和密度的分组预测模型。结果表明, 两个模型对条带性质的预测均表现出优异的预测性能, 该模型首次实现了杨氏模量的在线实时测定, 这对条带的工艺控制具有重要意义。

3.2 激光三角法在线预测固体分数

Lück 等[72]开发一种在线激光三角测量装置, 以粉末体积位移法为条带固体分数的参考方法, 建立了基于质量流量和 Midoux 模型的条带固体分数预测模型。质量流量预测方面, 采用激光三角测量装置在线监测辊压条带厚度 (图 5B), 通过稳态下空辊 ($\bar{x}_{empty}$) 与带条辊 ($\bar{x}_{ribbon}$) 的激光距离差计算平均厚度 $\Delta\bar{x}$。同步通过天平系统监测质量流量 ($\dot{m}$), 结合体积流量 ($\dot{v}$) 计算条带密度和条带固体分数。Midoux 模型[73,74]是 Johan-

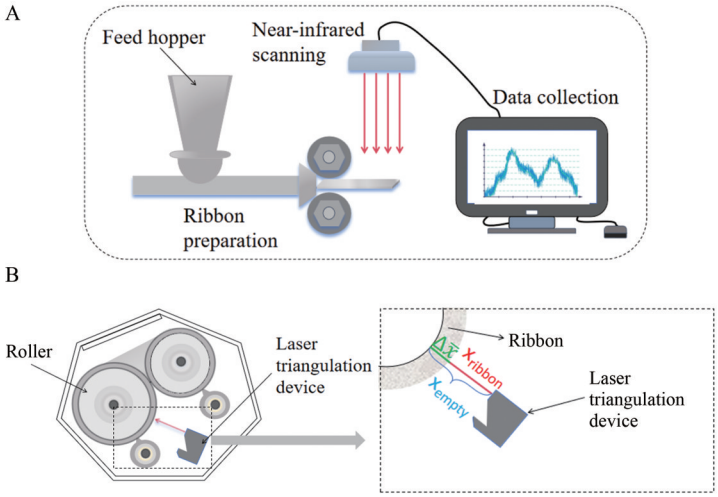


Figure 5 Application of online process analysis tools. A: Near-infrared light scanning ribbons online; B: Schematic diagram of on-line monitoring of laser triangulation device

son模型的简化而来, 该模型指出在辊轮间隙处的最大辊轮压力 (P_{max}) 为:

$$P_{max} = \frac{2SCF}{D} \times \sqrt{\frac{2K}{\pi S/D}} \quad (13)$$

其中, SCF是比压实力, D是辊轮直径, K是压缩指数, S是辊轮间隙宽度。通过P_{max}计算出Midoux模型中条带密度, 进而得出条带固体分数。

实验结果显示, 基于质量流量预测模型和基于Midoux模型的预测模型, 两种方法对固体分数都具有良好的预测能力, 并且Midoux模型不需要额外的质量测定, 对多组分配方体系展现出更高灵敏度, 易于在辊轮压实中实现。

4 总结与展望

辊压条带作为干法制粒过程中的关键质量属性和关键中间产品, 其性质决定了后续颗粒的密度、粒度分布、含量均匀性等。PAT与常规方法相结合, 能快速简便无损表征条带密度、固体分数和孔隙率等性质, 提高了干法制粒过程分析和质量控制水平。

PAT在表征性质方面仍存在诸多不足, 仍需进一步改进提高。首先, PAT大多只能应对单一材质的条带, 例如模型材料多是MCC这种可压性好、物料性质稳定的辅料, 建议增强多种辅料和药物处方的条带性质研究, 设法降低复杂物料对特征谱的干扰, 从而扩大方法的适用范围; 其次, PAT数据处理和选择缺乏详细研究, 预测模型多采用PCA、PLS等方法建立, 导致性质预测准确度不高, 建议增强数据的高维处理运算, 提取关键特征加入到预测模型中, 建立基于深度学习等算法的条带性质预测模型, 提升PAT检测的专属性; 最后, 条带的性质多局限在密度、固体分数、孔隙率等少数指标, 应尝试扩大性质表征范围, 将与条带质量和后期颗粒质量有关的性质均纳入到PAT检测中, 全面提高PAT检测水平。

作者贡献: 杨亚光负责综述撰写图表绘制工作; 安广涛、闫媛、赵玉、吴驿瑶协助参与文章修改; 祁东利完成文章修改、校对和审核。

利益冲突: 本文所有作者声明不存在利益冲突关系。

References

[1] Zhang QL, Luo YH, Xu GH, et al. Application of dry granulation technology in preparation of oral solid preparation of traditional Chinese medicine [J]. Mod Chin Med (中国现代中药), 2020, 22: 827-834.

[2] Wang Y, Wang YJ, Qi DL, et al. Prediction of formability of flavonoid extract granules by dry granulation based on design space and RBFNN [J]. China J Chin Mater Med (中国中药杂志), 2022, 47: 2955-2963.

[3] Huang ZY, Wang YJ, Qi DL, et al. Establishment of feedforward control model for dry granulation of polysaccharide components based on quality by design [J]. Chin J Exp Tradit Med Formulae (中国实验方剂学杂志), 2022, 28: 130-137.

[4] Wiedey R, Kleinebudde P. The density distribution in ribbons from roll compaction [J]. Chem Ing Tech, 2017, 89: 1017-1024.

[5] Zhong WJ, Huang YS. Optimization of dry granulation process of Jiawei Weiyanxiao tablets by response surface methodology [J]. J Guangdong Pharm Univ (广东药科大学学报), 2021, 37: 95-99.

[6] Vadaga AK, Gudla SS, Nareboina GSK, et al. Comprehensive review on modern techniques of granulation in pharmaceutical solid dosage forms [J]. Intell Pharm, 2024, 2: 609-629.

[7] Sandler N, Lammens RF. Pneumatic dry granulation: potential to improve roller compaction technology in drug manufacture [J].

Expert Opin Drug Deliv, 2011, 8: 225-236.

[8] Cao HH, Du RF, Feng Y, et al. Application progress in dry granulation technology of Chinese materia medica [J]. Chin Tradit Herb Drugs (中草药), 2013, 44: 2772-2776.

[9] Crowley ME, Hegarty A, McAuliffe MAP, et al. Near-infrared monitoring of roller compacted ribbon density: investigating sources of variation contributing to noisy spectral data [J]. Eur J Pharm Sci, 2017, 102: 103-114.

[10] Marinko N, Sedlářová I, Römerová S, et al. Method to determine envelope density for roller compacted ribbons by solid displacement of glass microspheres [J]. Powder Technol, 2024, 444: 120014.

[11] Wiedey R, Šibanc R, Kleinebudde P. Laser based thermo-conductometry as an approach to determine ribbon solid fraction off-line and in-line [J]. Int J Pharm, 2018, 547: 330-337.

[12] Khorasani M, Amigo JM, Sonnergaard J, et al. Visualization and prediction of porosity in roller compacted ribbons with near-infrared chemical imaging (NIR-CI) [J]. J Pharm Biomed Anal, 2015, 109: 11-17.

[13] Khorasani M, Amigo JM, Sun CC, et al. Near-infrared chemical imaging (NIR-CI) as a process monitoring solution for a production line of roll compaction and tableting [J]. Eur J Pharm Biopharm, 2015, 93: 293-302.

[14] Kashinath KP, Sanjay LR, Ashokbhai MK, et al. Continuous manufacturing based paradigm shift in pharmaceuticals production and current regulatory framework [J]. Chem Eng Res Des, 2025, 215: 1-22.

[15] Zhu WF, Shen Y, Deng P, et al. Application of process analysis technology in traditional Chinese medicine manufacturing industry [J]. China J Chin Mater Med (中国中药杂志), 2024, 49: 2299-2307.

[16] Zhou GR, Yang J, Zhang XR, et al. Research progress of process analysis technology in granulation [J]. J Jiangxi Univ Chin Med (江西中医药大学学报), 2022, 34: 106-111.

[17] Xiong HS, Zhang Q, Zhang SN, et al. Methodology and application of process analytical technology (PAT) for traditional Chinese medicine manufacturing: a review [J]. China J Chin Mater Med (中国中药杂志), 2023, 48: 22-29.

[18] McAuliffe MAP, Mahony GEO, Blackshields CA, et al. The use of PAT and off-line methods for monitoring of roller compacted ribbon and granule properties with a view to continuous processing [J]. Org Process Res Dev, 2015, 19: 158-166.

[19] Lim H, Dave VS, Kidder L, et al. Assessment of the critical factors affecting the porosity of roller compacted ribbons and the feasibility of using NIR chemical imaging to evaluate the porosity distribution [J]. Int J Pharm, 2011, 410: 1-8.

[20] Guo YW, Martinez L, Palanisamy A, et al. An evaluation of six techniques for measuring porosity of ribbons produced by roller compaction [J]. Int J Pharm, 2024, 667: 124855.

[21] Lillotte TD, Bebernik P, Keck J, et al. Laser triangulation as a fast and reliable method for determining ribbon solid fraction; focus on accuracy, precision, and measurement time [J]. Int J Pharm, 2021, 610: 121241.

[22] Yu LX, Amidon G, Khan MA, et al. Understanding pharmaceutical quality by design [J]. AAPS J, 2014, 16: 771-783.

[23] Michrafy A, Diarra H, Dodds JA, et al. Experimental and numerical analyses of homogeneity over strip width in roll compaction [J]. Powder Technol, 2011, 206: 154-160.

[24] Zhang JY, Pei CL, Schiano S, et al. The application of terahertz pulsed imaging in characterising density distribution of roll-compacted ribbons [J]. Eur J Pharm Biopharm, 2016, 106: 20-25.

[25] Ding Y, Dai HL, Jiang DL, et al. Research on rapid discrimination of different processing degrees of *Angelicae sinensis Radix* with yellow rice wine based on intelligent sense and near-infrared technology combined with chemometrics [J]. Chin Tradit Herb Drugs (中草药), 2025, 56: 68-78.

[26] Chen LP, Xu FF, Zhang X, et al. Near infrared prediction model for hardness of *Rhodiola grandiflora* tablets based on partial least square method [J]. Chin Tradit Herb Drugs (中草药), 2023, 54: 2446-2452.

[27] Fan LH, Fan WX, Wei ZQ, et al. Application status of near infrared spectroscopy combined with chemometrics in analysis of traditional Chinese medicine [J]. Chin J Exp Tradit Med Formulae (中国实验方剂学杂志), 2019, 25: 205-210.

[28] Chadha R, Haneef J. Near-infrared spectroscopy: effective tool for screening of polymorphs in pharmaceuticals [J]. Appl Spectrosc Rev, 2015, 50: 565-583.

[29] Tang M, Li XL, Li JQ, et al. Rapid discriminate analysis and quantitative analysis methods for carbonized Typhae Pollen using near infrared spectroscopy coupled with chemometrics [J]. Mod Tradit Chin Med Mater Med World Sci Technol (世界科学技术−中医药现代化), 2024, 26: 2385-2398.

[30] Zhang DW, Tian G, Xiong HS, et al. Granulation of Yangxue Qingnao granules in fluidized bed based on near-infrared spectroscopy [J]. China J Chin Mater Med (中国中药杂志), 2022, 47: 3806-3815.

[31] Liu QA, Xu FF, Zhang X, et al. Based on near-infrared spectroscopy technology and classification and regression trees algorithm to establish a prediction model of Tianshu tablets disintegration [J]. Chin Tradit Herb Drugs (中草药), 2021, 52: 4837-4843.

[32] Zhou LW, Wu ZS, Shi XY, et al. Research on NIR-CI parameters optimization of chlorpheniramine maleate tablets based on binary image and statistical measurement [J]. Spectrosc Spectral Anal (光谱学与光谱分析), 2014, 34: 2821-2826.

[33] Zhang N, Xu XY, Wang SH, et al. Application of chemical imaging based on vibration spectroscopy in pharmaceutical analysis [J]. Chin J Pharm Anal (药物分析杂志), 2023, 43: 1653-1663.

[34] Zhou LW, Wu ZS, Shi XY, et al. Rapid assessment of critical quality attributes of Chinese materia medica: visualization technology of near infrared chemical imaging [J]. Mod Tradit Chin

Med Mater Med World Sci Technol (世界科学技术–中医药现代化), 2014, 16: 2568-2574.

[35] Wang YF, Zhang YW, Wang JY, et al. Study on the evaluation method of commercial cataplasms spatial distribution homogeneity based on near-infrared chemical imaging (NIR-CI) technology [J]. China J Tradit Chin Med Pharm (中华中医药杂志), 2017, 32: 1830-1832.

[36] Amigo JM, Ravn C. Direct quantification and distribution assessment of major and minor components in pharmaceutical tablets by NIR-chemical imaging [J]. Eur J Pharm Sci, 2009, 37: 76-82.

[37] Yekpe K, Abatzoglou N, Bataille B, et al. Predicting the dissolution behavior of pharmaceutical tablets with NIR chemical imaging [J]. Int J Pharm, 2015, 486: 242-251.

[38] Khorasani M, Amigo JM, Bertelsen P, et al. Process optimization of dry granulation based tableting line: extracting physical material characteristics from granules, ribbons and tablets using near-IR (NIR) spectroscopic measurement [J]. Powder Technol, 2016, 300: 120-125.

[39] Wan YH, Dong XY, Wu YH, et al. Research progress of terahertz time-domain spectroscopy technology in coating detection [J]. Meas Control Technol (测控技术), 2023, 42: 22-35.

[40] Zeitler JA, Taday PF, Newnham DA, et al. Terahertz pulsed spectroscopy and imaging in the pharmaceutical setting- a review [J]. J Pharm Pharmacol, 2007, 59: 209-223.

[41] Haddad JE, Bousquet B, Canioni L, et al. Review in terahertz spectral analysis [J]. TrAC Trends Analyt Chem, 2013, 44: 98-105.

[42] Yang R, Chen G, Jiang L, et al. Progress in the application of terahertz spectroscopy in the field of fiber materials [J]. Applied Laser (应用激光), 2018, 38: 864-872.

[43] Jin YH, Zhu FX, Feng JX. Review of nondestructive testing of composites based on THz technology [J]. J Terahertz Sci Electron Inf Technol (太赫兹科学与电子信息学报), 2023, 21: 1295-1305.

[44] Dong RQ, Goodwin DJ, Nassar J, et al. Roller compaction: measuring ribbon porosity by terahertz spectroscopy and machine learning [J]. Int J Pharm, 2024, 667: 124852.

[45] Usamentiaga R, Venegas P, Guerediaga J, et al. Infrared thermography for temperature measurement and non-destructive testing [J]. Sensors (Basel), 2014, 14: 12305-12348.

[46] Meola C, Carlomagno GM. Application of infrared thermography to adhesion science [J]. J Adhes Sci Technol, 2006, 20: 589-632.

[47] Omar CS, Hounslow MJ, Salman AD. Implementation of an online thermal imaging to study the effect of process parameters of roller compactor [J]. Drug Deliv Transl Res, 2018, 8: 1604-1614.

[48] Wiedey R, Kleinebudde P. Infrared thermography - a new approach for in-line density measurement of ribbons produced from roll compaction [J]. Powder Technol, 2018, 337: 17-24.

[49] Wiedey R, Kleinebudde P. Potentials and limitations of thermography as an in-line tool for determining ribbon solid fraction [J]. Powder Technol, 2019, 341: 2-10.

[50] Kubala-Kukus A, Banas D, Braziewicz J, et al. X-ray spectrometry and X-ray microtomography techniques for soil and geological samples analysis [J]. Nucl Instrum Methods Phys Res Sect B, 2015, 364: 85-92.

[51] Fernandes JS, Appoloni CR, Fernandes CP. Accuracy evaluation of an X-ray microtomography system [J]. Micron, 2016, 85: 34-38.

[52] Ye LL, Xue YL, Wang YD, et al. Identification of ginseng root using quantitative X-ray microtomography [J]. J Ginseng Res, 2017, 41: 290-297.

[53] Vijayakumar J, Goudarzi NM, Eeckhaut G, et al. Characterization of pharmaceutical tablets by X-ray tomography [J]. Pharmaceuticals (Basel), 2023, 16: 733.

[54] Szulc-Musiol B, Duda P, Meisner M, et al. Hyperspectral and microtomographic analyses to evaluate the stability of quercetin and calcium effervescent tablets exposed to heat and ultraviolet radiation [J]. Processes, 2024, 12: 531.

[55] Markl D, Strobel A, Schlossnikl R, et al. Characterisation of pore structures of pharmaceutical tablets: a review [J]. Int J Pharm, 2018, 538: 188-214.

[56] Schomberg AK, Diener A, Wuensch I, et al. The use of X-ray microtomography to investigate the microstructure of pharmaceutical tablets: potentials and comparison to common physical methods [J]. Int J Pharm X, 2021, 3: 100090.

[57] Landis EN, Keane DT. X-ray microtomography [J]. Mater Charact, 2010, 61: 1305-1316.

[58] Carmignato S, Dreossi D, Mancini L, et al. Testing of X-ray microtomography systems using a traceable geometrical standard [J]. Meas Sci Technol, 2009, 20: 084021.

[59] Akseli I, Iyer S, Lee HP, et al. A quantitative correlation of the effect of density distributions in roller-compacted ribbons on the mechanical properties of tablets using ultrasonics and X-ray tomography [J]. AAPS PharmSciTech, 2011, 12: 834-853.

[60] Miguélez-Morán AM, Wu CY, Dong HS, et al. Characterisation of density distributions in roller-compacted ribbons using micro-indentation and X-ray micro-computed tomography [J]. Eur J Pharm Biopharm, 2009, 72: 173-182.

[61] Liang JY, You LR, Wen XQ, et al. Application of Kalman filtering algorithm in laser triangulation measurement [J]. Instrum Tech Sens (仪表技术与传感器), 2017, (11): 93-96.

[62] Liu SX, Zhu Y, Song YJ, et al. Development of 3D profile measurement system based on laser triangulation method [J]. Exp Technol Manag (实验技术与管理), 2017, 34: 85-88.

[63] Xing JC, Luo XH. Measurement of truck carriage volume with laser triangulation [J]. Infrared Laser Eng (红外与激光工程), 2012, 41: 3083-3087.

[64] Sun YC, Pang YJ, Bai ZX, et al. Application technology of laser triangulation [J]. Laser J (激光杂志), 2021, 42: 1-8.

[65] Liu Y, Shen XY, Chen AJ, et al. Measurement of round hole size based on line laser triangulation [J]. Applied Laser (应用激光), 2020, 40: 308-314.

[66] Sun C, Jia MN, Yu QF, et al. Calibration and epipolar rectification methods for stereo scheimpflug cameras [J]. Acta Optica Sinica (光学学报), 2022, 42: 110-116.

[67] Cai ZY, Chen M, Yang TX, et al. Grain volume measurement based on laser triangulation [J]. J Nanjing Agric Univ (南京农业大学学报), 2021, 44: 797-804.

[68] Libois Q, Lévesque-Desrosiers F, Lambert-Girard S, et al. Optical porosimetry of weakly absorbing porous materials [J]. Opt Express, 2019, 27: 22983-22993.

[69] Johansson J, Sparén A, Wikström H, et al. Optical porosimetry by gas in scattering media absorption spectroscopy (GASMAS) applied to roller compaction ribbons [J]. Int J Pharm, 2021, 592: 120056.

[70] Acevedo D, Muliadi A, Giridhar A, et al. Evaluation of three approaches for real-time monitoring of roller compaction with near-infrared spectroscopy [J]. AAPS PharmSciTech, 2012, 13: 1005-1012.

[71] Samanta AK, Karande AD, Ng KY, et al. Application of near-infrared spectroscopy in real-time monitoring of product attributes of ribbed roller compacted flakes [J]. AAPS PharmSciTech, 2013, 14: 86-100.

[72] Lück M, Klinken S, Kleinebudde P. Laser triangulation based in-line elastic recovery measurement for the determination of ribbon solid fraction in roll compaction [J]. J Pharm Sci, 2024, 113: 1020-1028.

[73] Sousa R, Valente PC, Nakach M, et al. Roller compaction scale-up made simple: an approximate analytical solution to Johanson's rolling theory [J]. J Pharm Sci, 2020, 109: 2536-2543.

[74] Lück M, De Saeger M, Kleinebudde P. Influence of roll speed during roll compaction and its effect on the prediction of ribbon solid fraction [J]. Pharmaceutics, 2022, 14: 2399.